International Journal of Bifurcation and Chaos, Vol. 6, No. 9 (1996) 1665–1671

PATTERNS, DEFECTS, AND EVOLUTION OF BÉNARD–MARANGONI CELLS

J. BRAGARD, J. PONTES* and M. G. VELARDE
Instituto Pluridisciplinar, Universidad Complutense de Madrid,
Paseo Juan XXIII No.1, E-28040 Madrid, Spain

Received December 12, 1995; Revised January 25, 1996

We consider a thin fluid layer of *infinite* horizontal extent, confined below by a rigid plane and open above to the ambient air, with surface tension linearly depending on the temperature. The fluid is heated from below. First we obtain the weakly nonlinear amplitude equations in specific spatial directions. The procedure yields a set of generalized Ginzburg–Landau equations. Then we proceed to the numerical exploration of the solutions of these equations in *finite* geometry, hence to the selection of cells as a result of competition between the possible different modes of convection.

1. Introduction

The onset of motion in heated fluid layers with a free upper surface has been extensively studied since the original experiments by Henri Bénard [1900]. A comprehensive introduction to Bénard convection is given in [Normand *et al.*, 1977; Velarde & Normand, 1980; Koschmieder, 1993]. Depending on the depth of the layer one distinguishes two basic mechanisms of instability. In sufficiently deep cells, or in cells in which the fluid is confined between rigid horizontal plates, the convective motion settles when buoyancy forces overcome viscous forces (Rayleigh–Bénard problem). Alternatively, in sufficiently shallow layers with an open surface, inhomogeneities in the surface-tension [Block, 1956; Pearson, 1958] are responsible for the onset of motion (Bénard–Marangoni problem). In both cases, the characteristic wavelength of the convective structure may be comparable to the depth of the cell or much larger, depending on whether the horizontal boundaries are good thermal conductors or not.

Despite the relative simplicity of the system and of the considerable effort devoted to understanding the observed phenomena, several questions remain open. In this work we address one of them, namely the question of pattern formation induced by surface-tension gradients in a finite system.

Specifically, in the case of surface tension gradient-driven convection, the system evolves mostly towards a hexagonal structure. The evolution of the selected pattern is described by a $(1+2)D$ set of amplitude equations that we have derived [Bragard & Velarde, 1995]. The paper is organized as follows: in Sec. 2 we sketch the derivation of the amplitude equations, in Sec. 3 we present a few results of the integration of these equations, and in Sec. 4 we provide some conclusions.

2. Amplitude Equations

Close to the instability threshold the system may be described by amplitude equations having

*On leave from Promon Engenharia ltda., Praia do Flamengo 154, 22210 Rio de Janeiro, Brazil.

a universal form [Landau, 1944; Stuart, 1958; Scanlon & Segel, 1967; Newell & Whitehead, 1969; Cross & Hohenberg, 1993]. The coefficients of these amplitude equations are specific to each instability, they depend on the dimensionless numbers of the problem containing fluid properties, boundary conditions and external forcing. Here we consider three dimensionless numbers:

$$Pr = \frac{\nu}{\kappa};\ Ma = -\frac{\partial\sigma}{\partial T}\frac{d\Delta T}{\kappa\eta};\ Bi = \frac{hd}{k} \qquad (1)$$

where ν and κ are, the kinematic and thermal diffusivity, respectively; σ is the surface tension, d is the thickness of the layer, ΔT is the temperature difference between the top free surface and bottom plate, η is the dynamic viscosity, h is the thermal surface conductance and k is the thermal conductivity of the fluid layer. The Marangoni number Ma is the ratio between the destabilizing force, e.g. the surface tension gradient and the stabilizing ones associated with thermal and viscous diffusion. The Prandtl number is an intrinsic characteristic of the fluid. The Biot number is a characteristic of the heat transfer at the boundaries, an infinite value of the Biot number corresponds to a perfectly conducting boundary, a zero value corresponds to a poorly conducting surface.

The equations that govern the system are the standard incompressible fluid mechanics equations: Navier–Stokes, continuity and energy equations that we take in dimensionless form:

$$\begin{aligned} \frac{\partial \mathbf{v}}{\partial t} + (\mathbf{v}\cdot\nabla)\mathbf{v} &= Pr(-\nabla p + \Delta\mathbf{v}) \\ \nabla\cdot\mathbf{v} &= 0 \\ \frac{\partial T}{\partial t} + \mathbf{v}\cdot\nabla T &= \Delta T \end{aligned} \qquad (2)$$

with the following boundary conditions: At the lower uniformly heated rigid plate:

$$\begin{aligned} \mathbf{v} &= 0 \\ \partial_z T - BiT &= \text{constant} \end{aligned} \qquad (3)$$

and at the top undeformable free surface:

$$\begin{aligned} w &= 0 \\ \partial_x\sigma &= \eta\partial_z u \\ \partial_y\sigma &= \eta\partial_z v \\ \partial_z T + BiT &= \text{constant}\,. \end{aligned}$$

We shall restrict consideration to the Boussinesq approximation [Pérez-Cordón & Velarde, 1975; Velarde & Pérez-Cordón, 1976].

To study the transition between the constant motionless conductive state and the convective state, and the dynamics of the structures that appear in this convective state, we use a multiple scale perturbation theory in the vicinity of the onset of the convection. We define a small parameter in order to separate the fast variables that describe the instability and the slow ones that are useful to describe the pattern dynamics. The details of the calculation are given elsewhere [Bragard & Velarde, 1995]. The temperature dependence reads as:

$$\begin{aligned} T = T(z)[&A_1(X, Y, \tau)\exp(i\mathbf{k^{(1)}}\cdot\mathbf{r}) \\ &+A_2\exp(i\mathbf{k^{(2)}}\cdot\mathbf{r}) \\ &+A_3\exp(i\mathbf{k^{(3)}}\cdot\mathbf{r}) + c.c.] \end{aligned} \qquad (4)$$

where $\mathbf{k^{(i)}}$ denotes three linearly critical wave vectors oriented at 120 degrees in the horizontal plane. The amplitude equations in the horizontal plane are (e.g. for A_1):

$$\begin{aligned} \alpha_t\partial_t A_1 = {} & \alpha_l\Delta A_1 + \alpha_q A_2^* A_3^* \\ & -\alpha_{cs}A_1|A_1|^2 - \alpha_{ci}A_1(|A_2|^2 + |A_3|^2) \\ & +\alpha_d(\mathbf{k^{(1)}}\cdot\nabla_x)^2 A_1 + i\beta_1(\mathbf{k^{(1)}}\cdot\nabla_x)(A_2^* A_3^*) \\ & +i\beta_2[A_2^*(\mathbf{k^{(2)}}\cdot\nabla_x)A_3^* + A_3^*(\mathbf{k^{(3)}}\cdot\nabla_x)A_2^*] \\ & +i\beta_3[A_3^*(\mathbf{k^{(2)}}\cdot\nabla_x)A_2^* + A_2^*(\mathbf{k^{(3)}}\cdot\nabla_x)A_3^*] \end{aligned} \qquad (5)$$

where

$$\begin{aligned} \alpha_l &= 0.0038 \\ \alpha_t &= 0.05 + 0.013\ Pr^{-1} \\ \alpha_q &= 0.0203 - 0.0046\ Pr^{-1} \\ \alpha_{cs} &= 0.016 + 0.0049\ Pr^{-1} + 0.00077\ Pr^{-2} \\ \alpha_{cs} &= 0.0217 + 0.003\ Pr^{-1} + 0.0018\ Pr^{-2} \\ \alpha_d &= 0.021 \\ \beta_1 &= 0.016 - 0.0041\ Pr^{-1} \\ \Delta &= Ma - Ma_c \end{aligned}$$

Similar equations appear for A_2 and A_3 (with circular permutation of the indices). We give the numerical value of the coefficient in the specific case of a poor conducting upper surface and good conducting lower plate. Other thermal conditions at the top and bottom change the numerical values of the coefficients. These equations are generalized Ginzburg–Landau equations with genuinely new advective

Table 1. Stable patterns according to the bifurcation parameter Δ.

$\Delta = Ma - Ma_c$	Stable Configurations
$\Delta < \Delta_c$	Conductive state
$\Delta_c < \Delta < 0$	Conductive state, Hexagons
$0 < \Delta < \Delta_1$	Hexagons
$\Delta_1 < \Delta < \Delta_2$	Hexagons, Rolls
$\Delta > \Delta_2$	Rolls

terms with β coefficients. For these equations there is no Lyapunov functional hence for some value of the β we may observe non-monotonic behavior. In the numerical simulations we shall concentrate on the two parameters Δ and β which are respectively the distance to the threshold and the coefficient of the advective terms.

The analytical study of Eq. (5) without spatial terms in *infinite* horizontal extent is known from Busse [1967]. The results of linear stability analysis of rolls and hexagons are summarized in Table 1.

The values of the constant for $Pr \to \infty$ are

$$\Delta_c = -\frac{\alpha_q^2}{4\alpha_l(\alpha_{cs} + 2\alpha_{ci})} \simeq -0.456$$

$$\Delta_1 = \frac{\alpha_q^2 \alpha_{cs}}{\alpha_l(\alpha_{cs} - \alpha_{ci})^2} \simeq 53.4$$

$$\Delta_2 = \frac{\alpha_q^2(2\alpha_{cs} + \alpha_{ci})}{\alpha_l(\alpha_{cs} - \alpha_{ci})^2} \simeq 179.2$$

As a consequence, two hysteresis cycles can be distinguished [Pérez-García *et al.*, 1990]. One occurs between the conducting state and the hexagonal pattern, in the interval $[\Delta_c, 0]$ and the second one between hexagons and rolls in the interval $[\Delta_1, \Delta_2]$. The existence of the first hysteretic loop has been observed in experiments [Koschmieder, 1993]. To our knowledge the transition from hexagons to rolls has not yet received experimental support. Busse's formulæ for space independent amplitude equations in *infinite* geometry provide a starting point for the exploration of the complete equation in *finite* geometry.

3. Numerical Results

In this section we present the results of five numerical simulations of the amplitude equations (5) in a square geometry, starting from random initial conditions (Cases I–IV) and starting with rolls (Case V). We solve the equations by means of a finite difference method using a semi-implicit splitting-type scheme.

A major question concerning the numerical procedure is to know *when* the system attains a steady state. We have used the method of Christov *et al.* [1995] based on the evaluation of a norm, which measures the rate of change of the distance between two successive states of the system, due to both the saturation and to the phase evolution of the pattern. Further details on this norm are given in Pontes *et al.* [1995].

Case I corresponds to $\Delta = 50$ and $\beta = 0.1$ (see Fig. 1). The system evolves to a stationary hexagonal pattern. The large value of β does not affect the pattern much. Simulations with $\beta = 0$ confirm that an increase of β only slightly distorts the pattern. Thus the advective terms in the amplitude equations do not play an important role in the case of an hexagonal structure. The fluid rises in the center of the cells in accordance with experimental observations [Koschmieder, 1993]. No defects are observed. The time evolution shown in Fig. 3 indicates how the system evolves to the stationary state.

Case II is for $\Delta = 75$ and $\beta = 0$ (see Fig. 2). For this value of Δ, the system is in the bistable region. Both hexagons and rolls are possible. The simulation displays the coexistence of these two structures. Figure 3 confirms the convergence to a steady state.

Case III was run with $\Delta = 150$ and $\beta = 0$ (see Fig. 4). We still increase the value of the bifurcation parameter Δ. For this value the rolls are the preferred structure. We reached this stationary state asymptotically (see Fig. 7). At the boundary, the rolls tend to be perpendicular to the sidewalls [Cross, 1982].

Case IV was run with $\Delta = 150$ and $\beta = 0.1$ (see Fig. 5). Increasing the parameter β to 0.02 we have not observed any changes with respect to Case III. For $\beta = 0.1$, Fig. 7 shows that the system does not reach a steady state. Beside the roll structure, defects appear moving through the system.

Case V was run with $\Delta = 150$ and $\beta = 0.1$ (see Fig. 6). Here a new simulation with the same parameter values is done but with rolls plus some superposed noise as the initial condition. First, the structure evolves to rolls without defects, but as time goes on the rolls start to bend and we

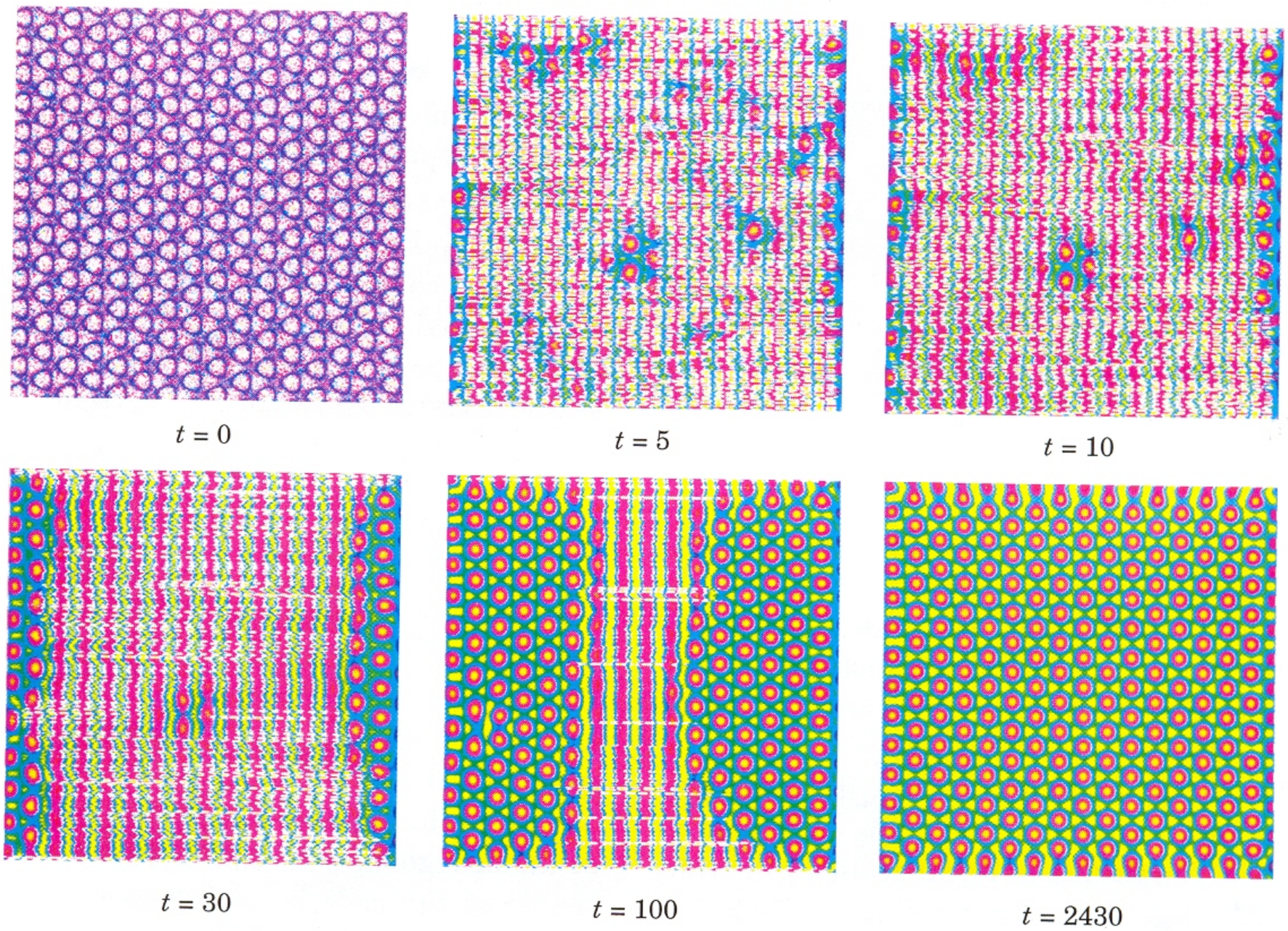

Fig. 1. Case I: Hexagons $\Delta = 50$; $\beta_i = 0.1$.

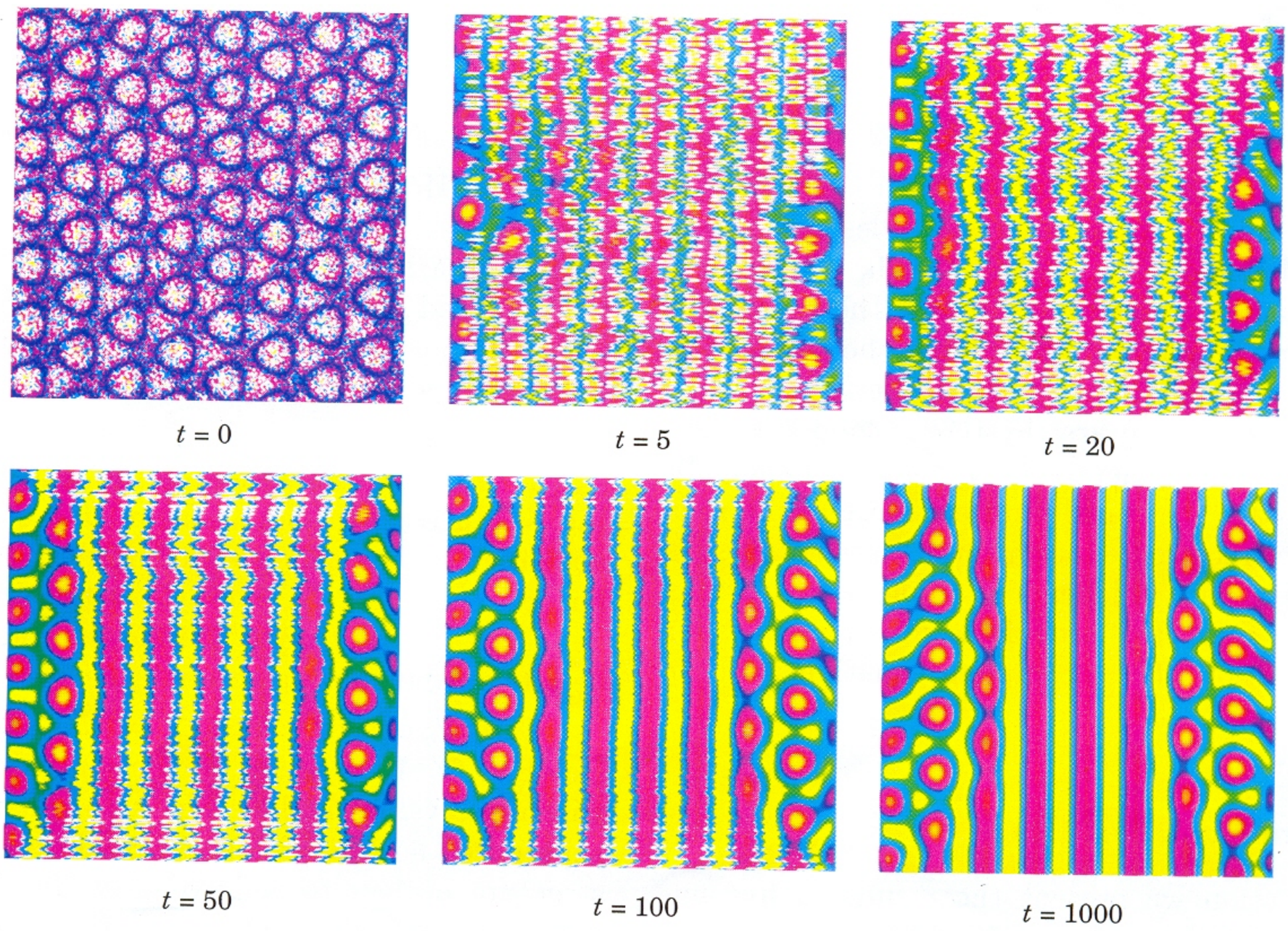

Fig. 2. Case II: Hexagons and Rolls $\Delta = 75$; $\beta_i = 0$.

observe an instability. This "secondary" instability looks like the Zig-Zag instability [Manneville, 1990]. Again, the system does not show evolution to a steady state.

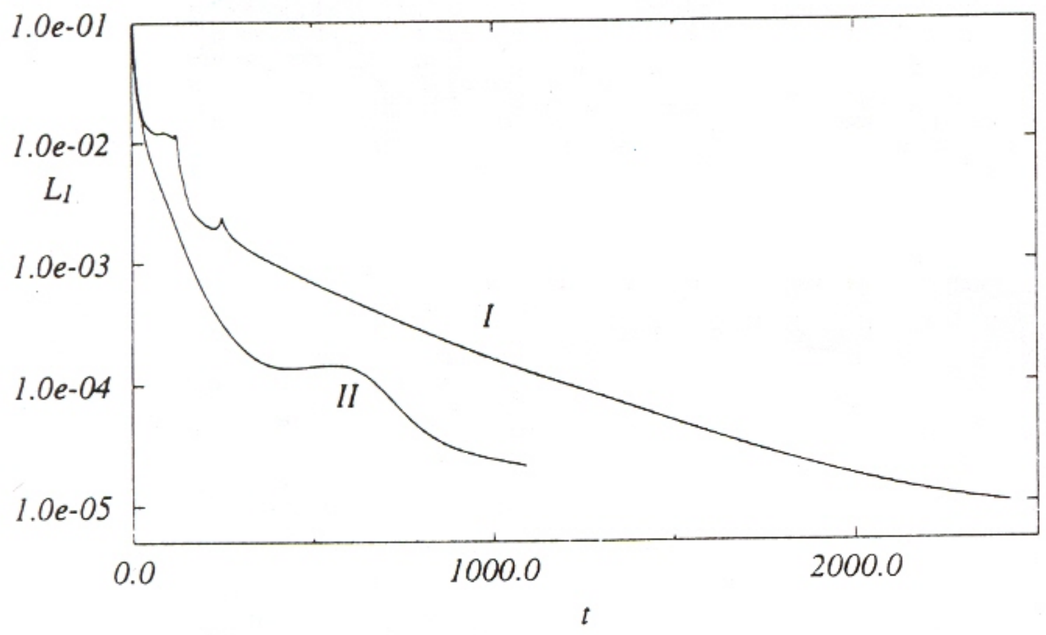

Fig. 3. $L_1 \times t$ curves of the evolution sequences for the cases (I, II).

4. Conclusions and Perspectives

Using amplitude equations, we have addressed the question of pattern formation in the Bénard–Marangoni convection. Past the onset of instability the hexagonal structure with fluid rising in the center of the cells is selected in agreement with experiment [Koschmieder, 1993]. For larger supercritical values, we numerically observed a transition between hexagons and rolls, a result also obtained analytically.

We have also studied the role of the new advective terms β in Eq. (5) in the non-potential evolution of the patterns. Specifically, we have shown that these terms do not affect much the hexagons but destabilize the roll pattern.

Recent numerical experiments done by Thess & Orzag [1995] do not support the transition hexagons-rolls but rather show an increase in the level of defects in the hexagonal structure. The fact that we have selected only three modes in the description of the pattern does not allow to observe these patterns with high level of defects.

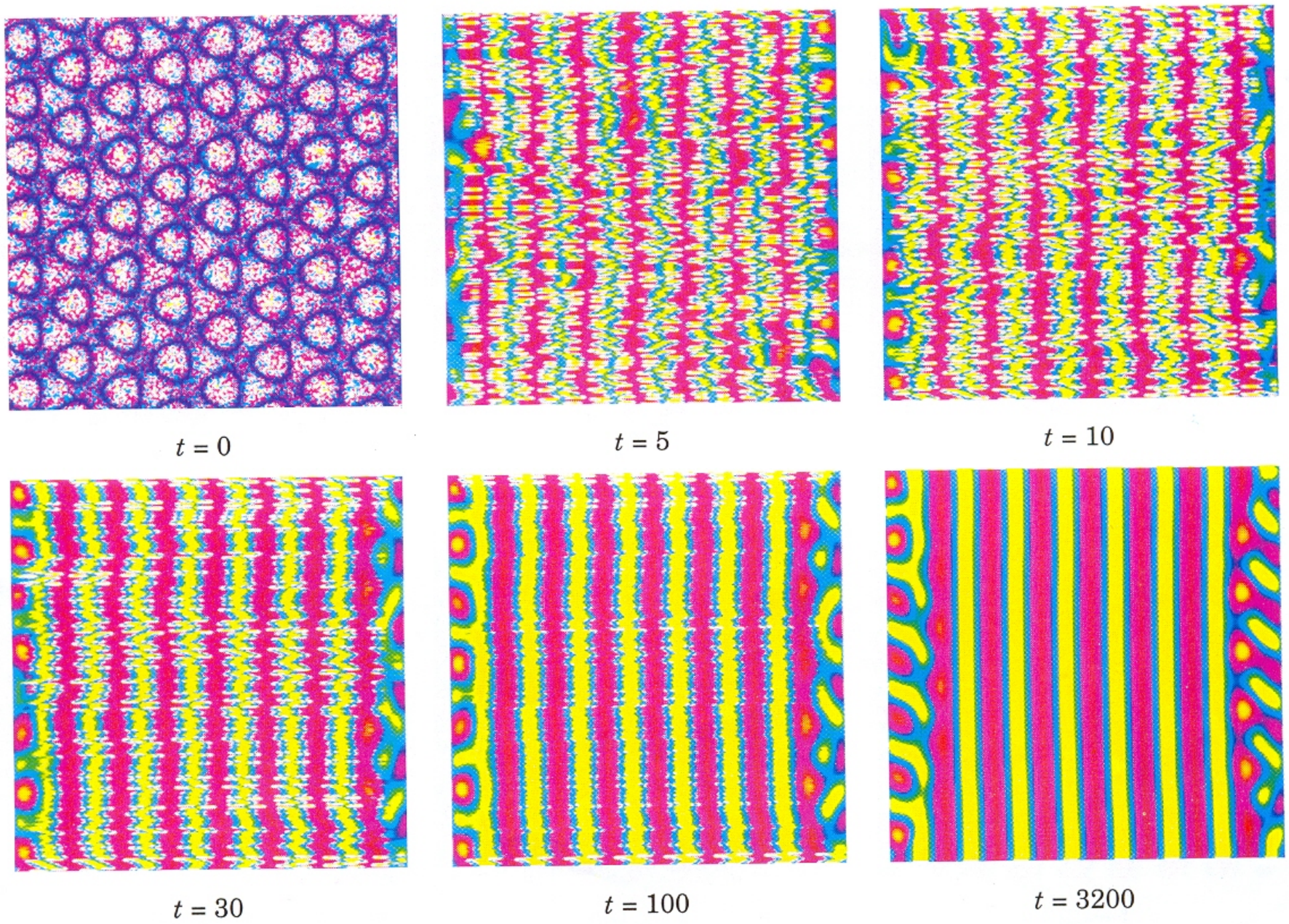

Fig. 4. Case III: Rolls $\Delta = 150$; $\beta_i = 0$.

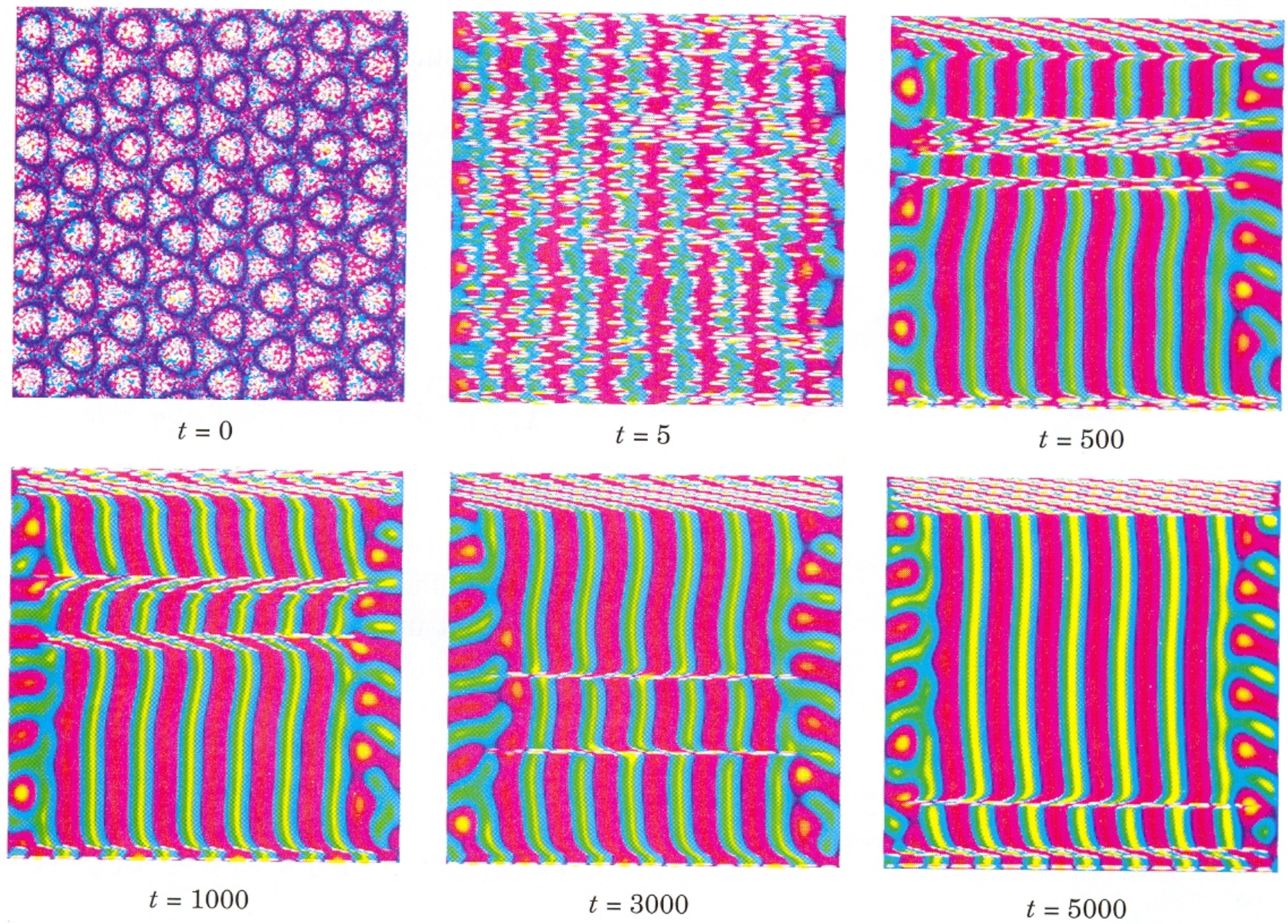

Fig. 5. Case IV: Rolls $\Delta = 150$; $\beta_i = 0.1$ (random initial condition).

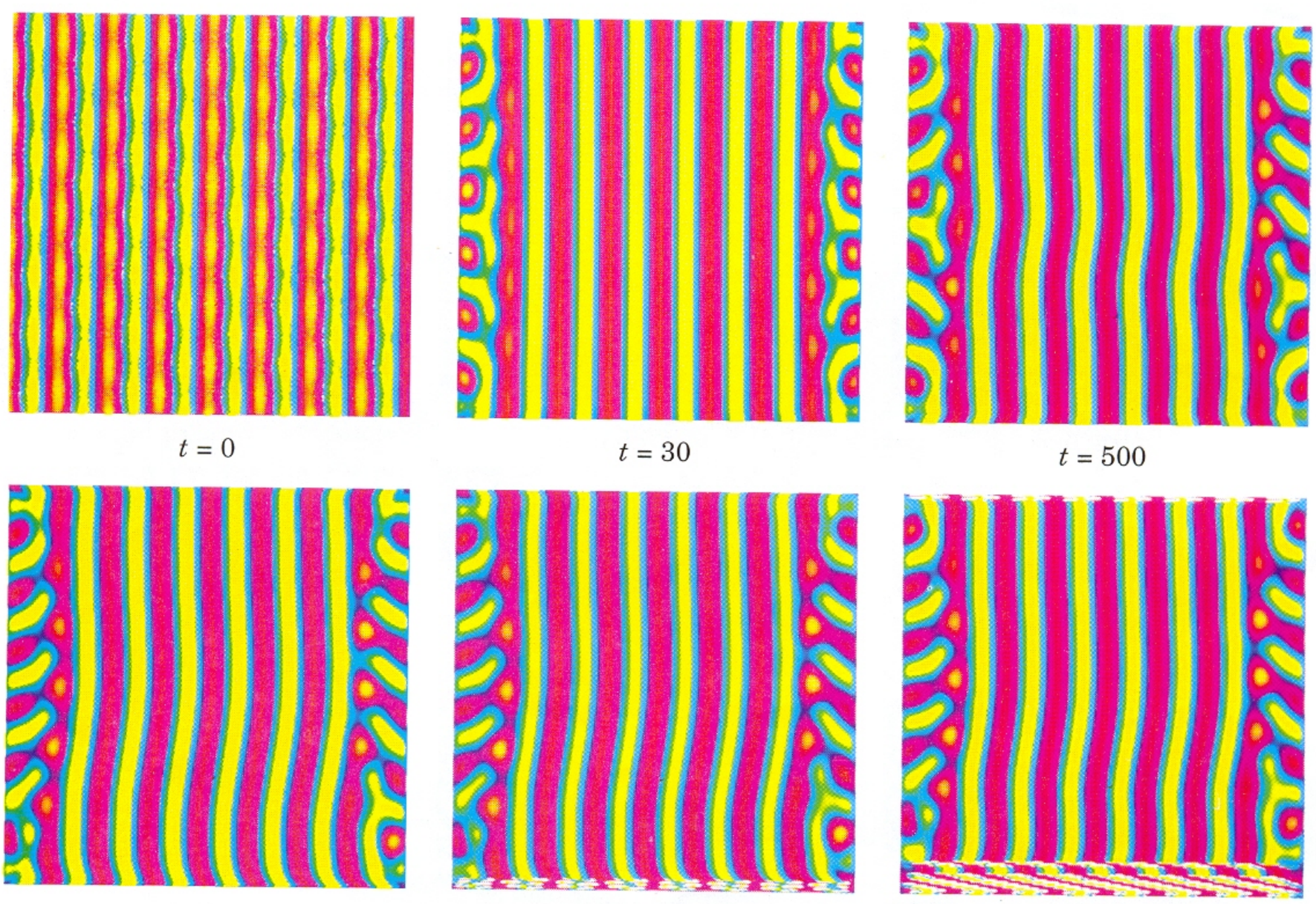

Fig. 6. Case V: Rolls $\Delta = 150$; $\beta_i = 0.1$ (rolls initial condition).

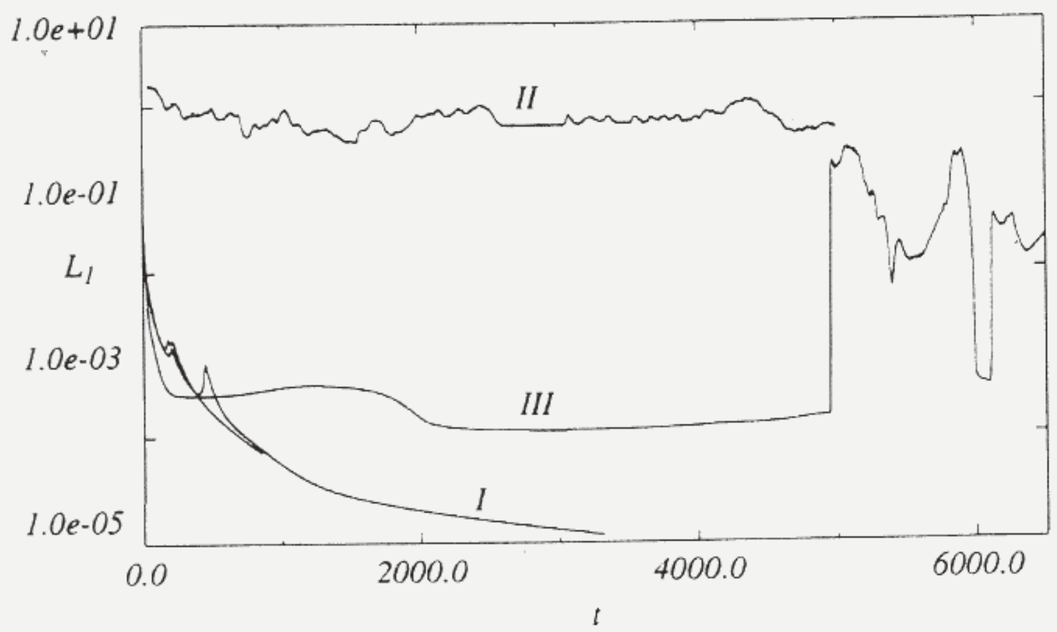

Norm $L_1 \times t$

Fig. 7. $L_1 \times t$ curves of the evolution sequences for the cases (III, IV, V).

Acknowledgments

The research has been supported by DGICYT (Spain) under Grant PB 93081, by Fundación "Ramon Areces" and by EU under Network Grant ERBCHRXCT 930107. The first author (J.B.) acknowledges support from the EU under Grant (ERBCHBICT 941046). The authors acknowledge Prof. C. I. Christov for his guidance in methods for numerical integration of PDE's.

References

Bénard, H. [1900] "Les tourbillons cellulaires dans une nappe liquide," *Rev. Gen. Sci. Pure Appl.* **11**, 1261–1309.

Block, M. J. [1956] "Surface tension as the cause of Bénard cells and surface deformation in a liquid film," *Nature* **178**, 650–651.

Bragard, J. & Velarde, M. G. [1995] "Bénard–Marangoni convection: Theoretical predictions about planforms and their relative stability," *J. Fluid Mech.*, (submitted).

Busse, F. H. [1967] "The stability of finite amplitude cellular convection and its relation to an extremum principle," *J. Fluid Mech.* **30**(4), 625–649.

Christov, C. I., Pontes, J. & Velarde, M. G. [1995] "Splitting methods for free-surface viscous fluids subject to thermal Marangoni effect," *Advanced Concepts and Techniques in Thermal Modeling*, Elsevier, Amsterdam, pp. 142–148.

Cross, M. C. [1982] "Ingredients of a theory of convective textures close to onset," *Phys. Rev.* **A25**(2), 1065–1076.

Cross, M. C. & Hohenberg, P. C. [1993] "Pattern formation outside of equilibrium," *Rev. Mod. Phys.* **65**, 851.

Koschmieder, E. L. [1993] *Bénard Cells and Taylor Vortices* (Cambridge University Press).

Landau, L. D. [1944] "On the problem of turbulence," *C.R. Acad. Sci. USSR* **44**, 311–314.

Manneville, P. [1990] *Dissipative Structures and Weak Turbulence* (Academic Press, San Diego).

Newell, A. C. & Whitehead, J. A. [1969] "Finite bandwidth, finite amplitude convection," *J. Fluid Mech.* **38**, 279–303.

Normand, C., Pomeau, Y. & Velarde, M. G. [1977] "Convective instability: A physicist approach," *Rev. Mod. Phys.* **49**(3), 581–624.

Pearson, J. R. A. [1958] "On convection cells induced by surface tension," *J. Fluid Mech.* **4**, 489–500.

Pérez-Cordón, R. & Velarde, M. G. [1975] "On the (nonlinear) foundations of Boussinesq approximation applicable to a thin layer of fluid," *J. Phys.* (*Paris*), **36**, 591–601.

Pérez-García, C., Pampaloni, E. & Ciliberto, S. [1990] "Finite-size effects in the transition from hexagons to rolls in convective systems," *Europhys. Lett.* **12**, 51–55.

Pontes, J., Christov, C. I. & Velarde, M. G. [1996] "Numerical study of patterns and their evolution in finite geometry," to appear in *Int. J. Bifurcation and Chaos.*

Scanlon J. W. & Segel, L. A. [1967] "Finite amplitude cellular convection induced by surface tension," *J. Fluid Mech.* **30**(I), 149–162.

Schatz, M. F., Van Hook, S. J., McCormick, W. D., Swift, J. B. & Swinney, H. L. [1995] "Onset of surface-tension-driven Bénard convection," to appear in *Phys. Rev. Lett.*.

Stuart, J. T. [1958] "On the nonlinear mechanics of hydrodynamic stability," *J. Fluid Mech.* **4**, 1–21.

Thess, A. & Orzag, S. A. [1995] "Surface-tension-driven Bénard convection at infinite Prandtl number," *J. Fluid Mech.* **283**, 201–230.

Velarde, M. G. & Normand, C. [1980] "Convection," *Sci. Am.* (7), 92–108.

Velarde, M. G. & Pérez-Cordón, R. [1976] "On the (nonlinear) foundations of Boussinesq approximation applicable to a thin layer of fluid. II. Viscous dissipation and large cell gap effects," *J. Phys.* (*Paris*), **37**, 176–182.